Journal of Alloys and Compounds 509 (2011) 5908–5912

Contents lists available at ScienceDirect

Journal of Alloys and Compounds

journal homepage: www.elsevier.com/locate/jallcom

Multiferroic and magnetoelectric properties of single-phase $Bi_{0.85}La_{0.1}Ho_{0.05}FeO_3$ ceramics

Xingquan Zhang[a], Yu Sui[a,b,*], Xianjie Wang[a], Jinhua Mao[a], Ruibin Zhu[a], Yi Wang[a], Zhu Wang[a], Yuqiang Liu[a], Wanfa Liu[c]

[a] Center for Condensed Matter Science and Technology (CCMST), Department of Physics, Harbin Institute of Technology, Harbin 150001, PR China
[b] International Centre for Materials Physics, Chinese Academy of Sciences, Shenyang 110016, PR China
[c] Dalian Institute of Chemical Physics, Dalian 116023, PR China

ARTICLE INFO

Article history:
Received 16 November 2010
Received in revised form 4 March 2011
Accepted 4 March 2011
Available online 12 March 2011

Keywords:
Multiferroic
$BiFeO_3$
Substitution
Magnetoelectric coupling

ABSTRACT

Single-phase $Bi_{0.85}La_{0.1}Ho_{0.05}FeO_3$ multiferroic ceramics were prepared by a rapid liquid sintering method. The ceramics exhibited an obvious ferroelectric loop with a remnant polarization of 11.2 μC/cm^2 and also showed weak ferromagnetism with the remnant magnetization of 0.179 emu/g at room temperature. A considerable enhancement of the polarization on magnetic poling and a dielectric anomaly in the vicinity of the antiferromagnetic transition temperature due to the intrinsic magnetoelectric coupling effect were observed in $Bi_{0.85}La_{0.1}Ho_{0.05}FeO_3$ ceramics. The dielectric constant for the $Bi_{0.8}La_{0.1}Ho_{0.05}FeO_3$ samples at room temperature decreases with increasing applied magnetic fields, and the coupling coefficient $(\varepsilon'(H)-\varepsilon'(0))/\varepsilon'(0)$ reaches −1.04% at H = 10 kOe.

1. Introduction

Recently, the perovskite compound $BiFeO_3$ (BFO), where ferroelectricity and antiferromagnetism coexist at room temperature, has been the subject of renewed interest [1,2]. Such multiferroic materials can present a strong coupling between the electric and magnetic order parameters, also called the magnetoelectric (ME) effect, which offers potential applications for new devices of magnetic storage as well as ferroelectric devices [3,4]. Below the ferroelectric Curie temperature of 837 °C, BFO possesses rhombohedral *R*3*c* symmetry characterized by antiphase $a^-a^-a^-$ octahedral tilting and off-center ionic displacements along $[1\,1\,1]_C$ direction of the parent cubic perovskite cell [5]. The mechanism for the ferroelectricity essentially comes from the long-rang ordering of dipolar moments on Bi site, in relation with the existence of Bi long pair and hybridization between Bi 6s and O 2p [6]. The spontaneous polarization of bulk BFO was expected to be 90–110 μC/cm^2 [7]. The antiferromagnetic ordering in bulk BFO is G-type below the Néel temperature (T_N), and a canted spin structure gives a spiral modulation with a periodicity of 62 nm, incommensurate with the crystal lattice [8]. In terms of functional properties, however, both single crystals and ceramics, at the exception of isolated reports [9,10], were far from showing the predicted ferroelectric polarization because of the presence of defects and the related high conductivity of processed materials. On the other hand, the long period modulated magnetic structure leads to cancellation of net macroscopic magnetization and hence inhibits the observation of linear ME effect. Several research groups have tried *A*-site (Bi-site) substitution by using rare-earth (RE) ions to modify the multiferroic properties of BFO in recent years [11–19]. Low-level substitutions of RE ions for bismuth have some interesting effects: (i) partial substitutions of RE ions (e.g., La^{3+}, Pr^{3+}, or Sm^{3+}) for bismuth help in eliminating the secondary phase along with a structural phase transition and improving ferroelectric properties of BFO. (ii) The introduction of RE ions in BFO seems to suppress the spin modulation and yield a weak ferromagnetism in the $Bi_{1-x}RE_xFeO_3$ compounds. Direct evidence of cycloid suppression in BFO was given via nuclear magnetic resonance measurements on La-substituted samples, which showed that the modulated structure disappears at x = 0.2, together with the structural transition from the rhombohedral (R3c) to an orthorhombic (C222) cell [20]. Furthermore, measurements of the dielectric constant as a function of magnetic field revealed the presence of ME coupling effect for $Bi_{0.8}Pr_{0.2}FeO_3$ [12], $Bi_{0.85}La_{0.15}FeO_3$ [21] and $Bi_{0.8}Dy_{0.2}FeO_3$ [22], which was chosen as representative, thus providing evidence of the possibility of substitution-induced spin cycloid suppression. Later investigations revealed that there is a strong dependence of the magnetic response with the size of the dopant ion [23]. It was found

* Corresponding author at: Center for Condensed Matter Science and Technology (CCMST), Department of Physics, Harbin Institute of Technology, Harbin 150001, PR China. Tel.: +86 451 86418403; fax: +86 451 86418403.
E-mail address: suiyu@hit.edu.cn (Y. Sui).

0925-8388/$ – see front matter © 2011 Elsevier B.V. All rights reserved.
doi:10.1016/j.jallcom.2011.03.037

that the most effective way to induce spontaneous magnetization in BFO should be related to the substitution with ions, possessing a large difference in ionic radius with respect to that of Bi^{3+}.

Even though lots of experimental works have been done on RE ions substituted bismuth ferrite, there are only a few investigations on Ho-substituted BFO in recent years. Compared with Bi^{3+} ion (radius = 1.17 Å), Ho^{3+} ion (1.041 Å) possesses a much smaller radius [24], which indicates that substitution of Ho^{3+} for Bi^{3+} in BFO would cause a more significant structural distortion and suppress of spin cycloid in BFO effectively. In addition, as magnetically active ion, substitution Ho^{3+} ion for Bi^{3+} ion could result in additional magnetic interactions and ordering, and further enhance the effect of *A*-site substitution in BFO. The Ho-substituted nanocrystalline BFO indeed exhibits spontaneous magnetization at room temperature [25]. However, the dielectric, ferroelectric, and ME properties of Ho-substituted BFO were not reported. In this paper, we prepared single-phase $Bi_{0.85}La_{0.1}Ho_{0.05}FeO_3$ (BLHFO) ceramics and investigated their structural, ferroelectric, magnetic, and ME properties. A small amount of lanthanum is added to stabilize the perovskite BFO phase as reported by Palkar et al. for Tb substituted BFO [26]. Single-phase BFO and $Bi_{0.9}La_{0.1}FeO_3$ (BLFO) samples were also prepared and characterized for comparison.

2. Experimental

Polycrystalline BFO, BLFO, and BLHFO ceramics were prepared by the rapid liquid phase sintering method [27]. High purity powders of Bi_2O_3, La_2O_3, Ho_2O_3, and Fe_2O_3 were used as starting materials. After weighing and ball milling, the mixed powders were dry pressed into small discs with a diameter of ~8 mm and thickness of ~1 mm. These discs were dehydrated at 150 °C for 12 h in a vacuum chamber before being sintered at a relatively high temperature for a short time of 20 min. The optimized synthesized temperatures were 830 °C, 850 °C and 860 °C for BFO, BLFO, and BLHFO ceramics, respectively. Crystallographic structure analysis was performed by X-ray diffraction (XRD) using a Bede D^1 XRD diffractometer with Ni filtered Cu Kα (λ = 0.15406 nm) radiation. Differential thermal analysis (DTA) was performed with a SETARAM model No. TG/DTA-92B Jupiter system under nitrogen atmosphere with a heating rate of 10 °C/min. Differential scanning calorimetry (DSC; TA Instruments 2920, USA) was utilized to determine the T_N with a heating rate of 10 °C/min under nitrogen atmosphere. The ferroelectric hysteresis loops and leakage currents of the samples were measured using a Precision Premier Workstation (Radiant Technology, USA). For the measurements of electrical properties, the disks (6 mm diameter, 0.4–0.5 mm thick) were carefully polished and Ag electrodes were applied on both surfaces to form metal-insulator-metal capacitors. The polarization hysteresis loops were acquired at a frequency of 100 Hz. Dielectric measurements were carried out in the frequency range (100 Hz–1 MHz) using an impedance analyzer (HP 4194 A). Magnetic properties of the samples were obtained using the physical properties measurement system (PPMS) of Quantum Design.

3. Results and discussion

Fig. 1 shows the XRD patterns of BFO, BLFO and BLHFO ceramics. It can be seen that all the samples exhibit single-phase characteristics with no trace of other impurity phases (e.g., La_2O_3, Ho_2O_3, $Bi_2Fe_4O_9$, etc.) within the uncertainty of XRD. All the diffraction peaks in each pattern of BLFO and BLHFO ceramics can be indexed according to the crystal structure of pure BFO. Using the values of Shannon's ionic radii, we calculated that the radius ratio of Ho^{3+} ion to Bi^{3+} ion is 0.88 and the radius ratio of La^{3+} ion to Bi^{3+} ion is 1. These two values are higher than 0.59, which is the criterion of the ratio of the atomic (ionic) radius of the solute to solvent of forming interstitial solid solution [28]. So it would be difficult for La^{3+} and Ho^{3+} to enter the interstitial site of the BFO crystal; it is very likely for La^{3+} and Ho^{3+} to replace the Bi^{3+} site instead. The shift in peaks in XRD further confirms the substitution. If La^{3+} or Ho^{3+} entered the interstitial site of the BFO crystal, the diffraction peaks would shift distinctly towards the lower angles based on Bragg's law [29]. Contrarily, a slight shift in peaks to a greater 2θ angle is observed when Ho^{3+} ions are introduced in BFO. This indicates the substitution of the smaller Ho^{3+} ion for the larger Bi^{3+} ion. While only La^{3+} is doped into BFO, the position of the peaks has no shift. This also indicates that La^{3+} ions replace the Bi^{3+} ions. Careful inspection of the XRD patterns also reveals that (shown in the inset of Fig. 1) the doubly split peaks of BFO in the 2θ ranges of 31–33° and 38–41° merge partially to form a broadened peak in BLHFO. Such a behavior indicates the propensity of the structure to undergo significant structural distortion by Ho substitution [21]. The calculated lattice parameters of these ceramics are: for BFO, $a = 5.5797(3)$ Å, $c = 13.8593(2)$ Å, for BLFO, $a = 5.5722(2)$ Å, $c = 13.8160(1)$ Å, and for BLHFO, $a = 5.5672(2)$ Å, $c = 13.8038(4)$ Å.

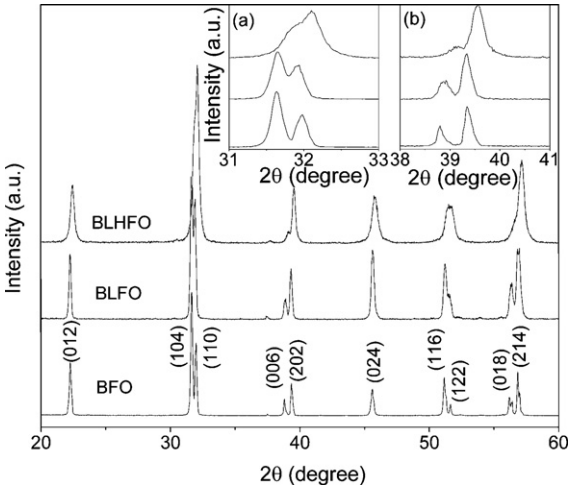

Fig. 1. X-ray diffraction patterns of the BFO, BLFO and BLHFO ceramics with magnification patterns showing in insets for different 2θ ranges of about (a) 31–33 and (b) 38–41.

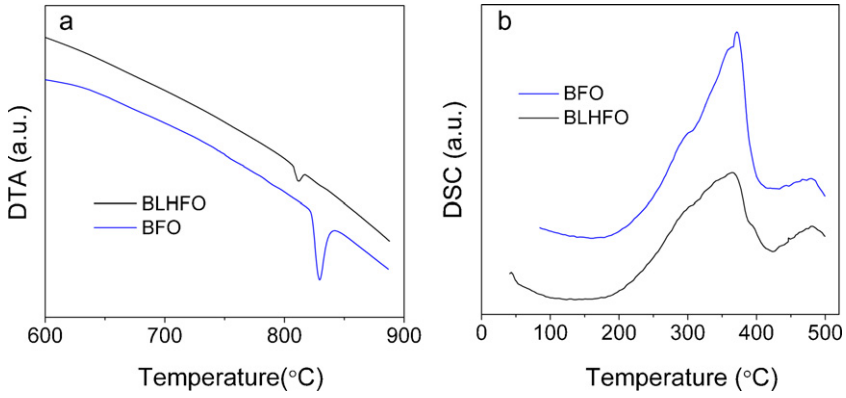

Fig. 2. (a) Differential thermal analysis (DTA) traces identifying the transitions from ferroelectric to paraelectric phase (T_C) of BFO and BLHFO samples. (b) Differential scanning calorimetry (DSC) traces identifying the Néel temperature (T_N) of BFO and BLHFO samples.

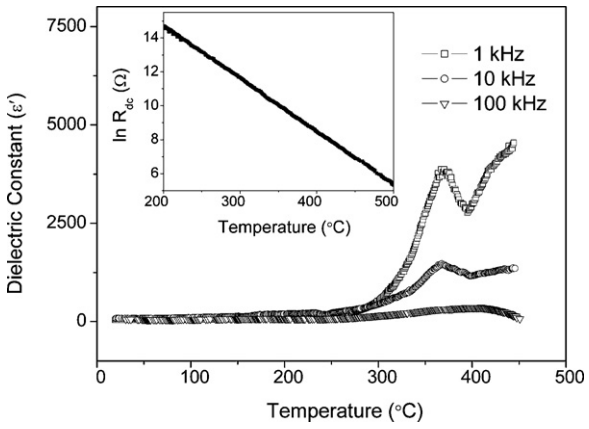

Fig. 3. Temperature dependence of relative dielectric constant for the BLHFO sample. The inset shows the temperature dependence of dc resistance of BLHFO across T_N.

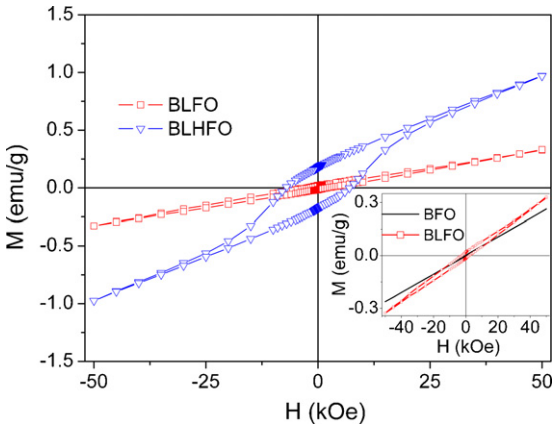

Fig. 4. Field dependence of magnetization (M–H) for BLFO and BLHFO samples measured at room temperature. The inset shows the magnetic hysteresis plots for the BLFO sample in a reduced scale. For comparison, the M–H hysteresis loop of the pure BFO sample is also shown in the inset of Fig. 4.

La and Ho substitution has not affected the crystalline structure of the parent compound BFO, which is important for the ferroelectric properties of the compounds. The existence of ferroelectricity and the corresponding Curie temperature (T_C) for these ceramics were determined using DTA. Fig. 2(a) shows the DTA curves of BFO and BLHFO samples for heating cycles in the 600 °C to 880 °C temperature interval. Endothermic peaks signifying the first-order phase transition could be identified in the heating cycle. For pure BFO, a strong peak is observed at ~830 °C consistent with the reported T_C [2], and shifts down to 809 °C for BLHFO. The decrease in ferroelectric transition temperature of La and Ho substituted BFO may be attributed to site disorder and defects generated due to substitution [30].

Fig. 2(b) shows the DSC curves of BFO and BLHFO samples revealing the magnetic transition temperature (T_N). The DSC peaks exhibit an apparent λ-type, indicating a second-order transition. Thus the observed DSC peaks correspond to the antiferromagnetic–paramagnetic transition. T_N of BLHFO defined by the peak of the curve is observed at 370 °C consistent with that of pure BFO, indicating that La and Ho substitution does not influence the T_N of BFO. This could be due to the fact that Bi-site is responsible for ferroelectric nature and Fe-site is responsible for magnetic properties of BFO. Incidentally, a dielectric anomaly has also been observed near the magnetic transition temperature T_N for BLHFO (shown in Fig. 3). Such a small dielectric anomaly in the vicinity of T_N has been reported for bulk and thin films of BFO based systems [31,32]. Generally, such an anomaly in $\varepsilon'(T)$ may originate from different factors, such as an extrinsic resistive component of the dielectric response together with the Maxwell–Wagner effect [33], which can lead to an artifact in the dielectric enhancement produced by the carrier migration to the interfaces within any heterogeneous semiconductor, and intrinsic multiferroic coupling via the magnetoelastic effect [32]. To verify the origin of the anomaly in $\varepsilon'(T)$ observed in the BLHFO samples, the temperature dependence of dc resistance across T_N was also measured, as shown in the inset of Fig. 3. It can be found that no anomaly can be observed in the dc resistance near T_N, compared with the distinct anomaly in $\varepsilon'(T)$ near T_N, implying that the role of the resistive part of the dielectric response is insignificant. This helps us to exclude the possibility of the resistive origin of the dielectric anomaly near T_N. On the other hand, lattice distortion and unit cell parameter anomalies have been observed at the magnetic transition temperature in BFO based systems [32]. Based on these facts we can attribute the anomaly in $\varepsilon'(T)$ near T_N to the intrinsic ME coupling in the BLHFO samples.

The introduction of Ho^{3+} on the perovskite A-site is expected to modify the magnetic properties of BFO because of the effect of unpaired electrons on Ho^{3+} which could result in additional magnetic interactions and ordering, and the modifications on the structure. Fig. 4 shows the room temperature magnetization hysteresis (M–H) loops of the BLFO and BLHFO samples. The BLFO samples display a narrow hysteresis loop with a small remnant magnetization of 0.018 emu/g instead of the antiferromagnetic characteristic in bulk BFO (as shown in the inset of Fig. 4), which is consisted with other reports and attributed to the fact that the spiral spin order is partially destroyed due to the La substitution [20]. In comparison, the BLHFO samples show clear hysteretic behavior with a remnant magnetization of 0.179 emu/g under 50 kOe, which is about 10 times larger than that of BLFO. Hence Ho substitution plays the dominant role towards the increase in magnetization. The enhanced magnetization in BLHFO at room temperature could be result from the structural distortion introduced by the Ho^{3+} ion with a smaller ionic radius than Bi^{3+} and La^{3+}, which destroys the spiral spin modulation in BFO effectively.

Fig. 5(a) and (b) shows the temperature dependent magnetization for the BFO, BLFO and BLHFO samples and the M–H response taken at T = 5 K. In contrast to the BFO and BLFO samples, a sharp increase in the magnetization takes place for the BLHFO samples with decreasing temperature, but no saturation of the magnetization is observed even at T = 5 K. The values of magnetization M at the magnetic field of 50 kOe for the BFO, BLFO, and BLHFO samples are: 0.301 emu/g, 0.389 emu/g, and 4.67 emu/g, respectively. It can be found that the magnetization M of BLHFO at 50 kOe is significantly larger than that of BFO and BLFO. These behaviors should attribute to the contribution from the side of the Ho^{3+} ions. Although La^{3+} and Ho^{3+} are both RE ions, La^{3+} ion is a diamagnetic ion, while Ho^{3+} is a magnetically active ion and has a large magnetic moment. When Bi^{3+} ions are substituted only by La^{3+} ions, the enhancement of magnetization in BLHFO could be attributed to suppression of the spiral spin modulation of BFO induced by the substitution effect. While Bi^{3+} was substituted by an amount of Ho^{3+} ions, the interaction between the spins of the Ho^{3+} ion and the Fe^{3+} ion, which, to some extent, decouples the antiferromagnetic interactions between the Fe^{3+} ions and thus provides a significant enhancement of the magnetization at low temperatures [15].

It is known that well saturated ferroelectric loops in pure BFO are difficult to obtain due to the inherently high coercive field and high leakage currents. The relatively higher leakage of BFO is known to be attributed to the existence of oxygen vacancies and Fe^{2+}, both of which can form impurity energy levels in the band gap of BFO [34]. Recently, oxygen vacancy, rather than Fe^{2+}, is found to make more contribution towards the high leakage current [35,36], which

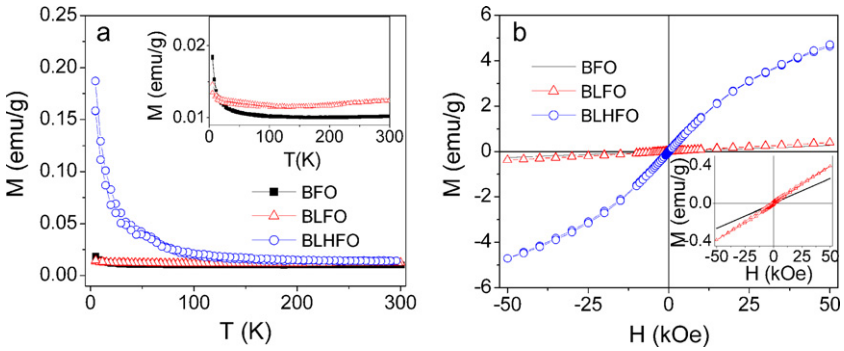

Fig. 5. (a) Temperature dependence of the magnetization (*M*–*T*) for the BFO, BLFO, and BLHFO samples measured at 1 kOe. The inset shows the *M*–*T* curves for BFO and BLFO samples in a reduced scale. (b) Field dependence of magnetization (*M*–*H*) for BLFO and BLHFO samples measured at 5 K. The inset shows the *M*–*H* hysteresis loops for BFO and BLFO samples in a reduced scale.

could dramatically enhance the breakdown voltage. Previous works [10,12] revealed that doping of RE ions can suppress the formation of oxygen vacancies in BFO ceramics and the leakage current of BFO. Fig. 6(a) shows the electric field dependence of leakage current density (*J*–*E*) for the BFO, BLFO, and BLHFO samples. Indeed, La and Ho substitution produces significant decrease in the leakage current density of the ceramics. At an applied electric field of 20 kV/cm, the leakage current density of BLHFO is about 6.9×10^{-8} A/cm^2, which is approximately three and two order of magnitude less than that of BFO (3.4×10^{-5} A/cm^2) and BLFO (1.4×10^{-6} A/cm^2), respectively, showing clearly that the leakage current can be effectively reduced by Ho substitution. Fig. 6(b) shows the room temperature polarization hysteresis (*P*–*E*) loops of the BFO, BLFO, and BLHFO samples measured at a frequency of 100 Hz. The *P*–*E* loop of the pure BFO is rounded, and it would be easily breakdown under a high maximum electric field due to probably the high leakage current in this sample. The shape of the *P*–*E* loop of the BLFO is improved due to La doping. Furthermore, a rectangular-like loop with large P_r is observed in the La and Ho substituted BLHFO ceramics. Under a maximum electric field of 135 kV/cm, the coercive field (E_c) value of the BLHFO ceramics is 78 kV/cm, and the P_r value is 11.2 μC/cm^2, which is comparable to the enhanced polarizations of modified BFO bulk ceramics reported in the literature [13,15]. This large P_r value for the BLHFO may be attributed to the possible lower concentration of oxygen vacancies induced by Ho substitution, which alleviates the domain pinning effect in the ceramics [37].

The magnetodielectric (MD) effect, which signifies the variation of the relative dielectric permittivity by a static bias magnetic filed, is commonly used to describe the ME coupling in multiferroics [38]. Here, the MD is defined as the following formula:

$$\mathrm{MD} = \frac{\varepsilon'(H) - \varepsilon'(0)}{\varepsilon'(0)} \quad (1)$$

where MD (%) is magnetodielectric coefficient, and $\varepsilon'(H)$ and $\varepsilon'(0)$ are the dielectric constants at applied magnetic field and zero field, respectively. The MD effect was studied in BLHFO samples. The measurement was repeated three times, and the average values were shown in Fig. 7(a). Here the dielectric constant is found to decrease with increasing applied magnetic field, giving the largest negative coupling coefficient of −1.04% at the highest magnetic field of 10 kOe. This value is comparable to the value obtained by Wang et al. in Ba-doped BFO ceramics [39]. It should be noted that the MD can also be induced by the magnetoresistance combined with the Maxwell–Wagner effect as suggested by Catalan [36]. In order to see the influence of magnetoresistance on the MD effect observed in Fig. 7(a), the resistivity of the BLHFO sample was measured as a function of applied magnetic field. The resistivity value at room temperature was of the order of 10^{10} Ωcm and no effect of magnetic field was found up to 8 kOe. Therefore, the MD effect observed in BLHFO is expected to be an intrinsic effect of the samples. To further demonstrate the coupling between electric and magnetic polarizations in BLHFO, the effect of magnetic poling on the ferroelectric hysteresis loop measured at room temperature is plotted in Fig. 7(b). After poling at 10 kOe dC magnetic field for 30 min, the *P*–*E* loop showed an enhancement in the P_r from 11.2 to 13.8 μC/cm^{-2}. Such a behavior was previously reported in BFO based systems [15,34] as a signature of the ME coupling occurring in the samples. According to Palkar et al. [26], the ME coupling observed in our samples could be qualitatively understood as follows. In multiferroics, when a magnetic field is applied, the materials will be strained. Due to the coupling between the magnetic and ferroelectric domain, the strain will induce stress and then generate an electric field on the ferroelectric domain, leading to the increase in the polarization value and the change in the dielectric constant.

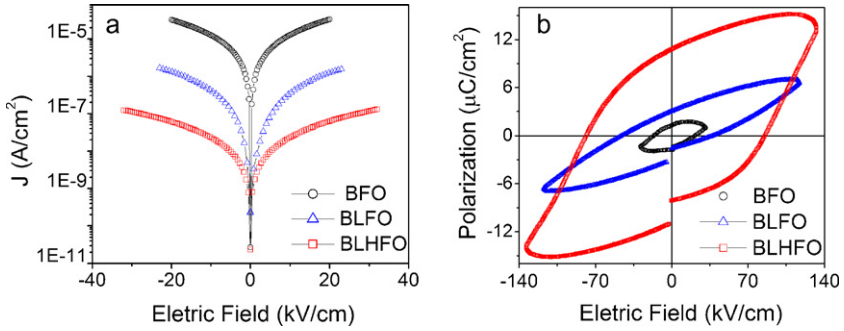

Fig. 6. (a) The leakage current density–electric field (*J*–*E*) behaviors and (b) ferroelectric hysteresis loops (*P*–*E*) measured for the BFO, BLFO, and BLHFO samples at room temperature.

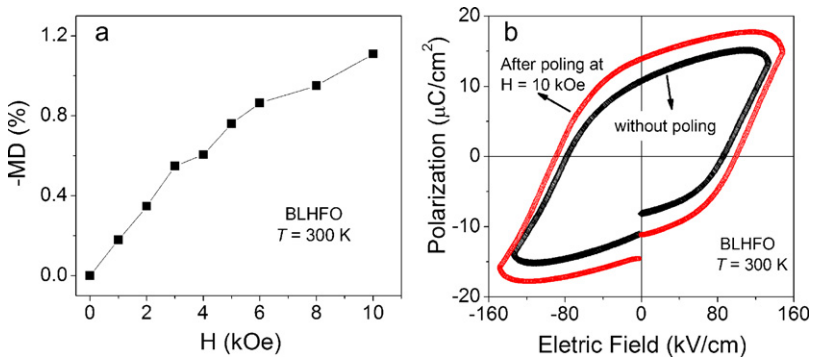

Fig. 7. (a) Magnetodielectric (MD) effect of the BLHFO sample measured at 3 kHz frequency at room temperature. (b) Ferroelectric hysteresis loops measured at a frequency of 100 Hz before and after poling at a dc magnetic field of 10 kOe for the BLHFO sample.

4. Conclusions

In conclusion, single-phase BLHFO multiferroic ceramics were prepared by a rapid liquid sintering method and a detailed study of electrical and magnetic properties of the ceramics was reported. BLHFO ceramics exhibit a large remnant polarization with high ferroelectric T_C and significantly improved magnetization from that of BFO. An anomaly is observed in the dielectric constant near T_N due to the intrinsic ME coupling in BLHFO. The increases in the remanent polarization after poling in the magnetic field and the decrease in the dielectric constant with increasing applied magnetic fields indicate ME coupling between electric and magnetic polarizations in BLHFO at room temperature. Based on these results, we conclude that Ho is a potential candidate to be substituted in BFO multiferroic material systems, which certainly helps to enhance multiferroic properties and possible multifunctional applications.

Acknowledgements

This work is supported by the National Natural Science Foundation of China (grant nos. 50672019 and 10804024). The project was sponsored by the Scientific Research Foundation for the Returned Overseas Chinese Scholars, State Education Ministry. The project (HIT. NSRIF.2009056) was supported by the Natural Scientific Research Innovation Foundation in Harbin Institute of Technology.

References

[1] J. Wang, J.B. Neaton, H. Zheng, V. Nagarajan, S.B. Ogale, B. Liu, D. Viehland, V. Vaithyanathan, D.G. Schlom, U.V. Waghmare, N.A. Spaldin, K.M. Rabe, M. Wuttig, R. Ramesh, Science 299 (2003) 1719.
[2] G. Catalan, J.F. Scott, Adv. Mater. 21 (2009) 2463.
[3] M. Fiebig, J. Phys. D 38 (2005) R123.
[4] K.F. Wang, J.M. Liu, Z.F. Ren, Adv. Phys. 58 (2009) 321.
[5] H.D. Megaw, C.N.W. Darlington, Acta Crystallogr. Sect. A: Found Crystallogr. 31 (1975) 161.
[6] N.A. Hill, J. Phys. Chem. B 104 (2000) 6694.
[7] J.B. Neaton, C. Ederer, U.V. Waghmare, N.A. Spaldin, K.M. Rabe, Phys. Rev. B 71 (2005) 014113.
[8] I. Sosnowska, T. Peterlin-Neumaier, E. Steichele, J. Phys. C: Solid State Phys. 15 (1982) 4835.
[9] D. Lebeugle, D. Colson, A. Forget, M. Viret, Appl. Phys. Lett. 91 (2007) 022907.
[10] G.L. Yuan, S.W. Or, J. Appl. Phys. 89 (2006) 3136.
[11] N. Kumar, N. Panwar, B. Gahtori, N. Singh, H. Kishan, V.P.S. Awana, J. Alloys Compd. 501 (2010) L29.
[12] P. Uniyal, K.L. Yadav, J. Phys. Condens. Matter. 21 (2009) 405901.
[13] Y.H. Lin, Q.H. Jiang, Y. Wang, C.W. Nan, L. Chen, J. Yu, Appl. Phys. Lett. 90 (2007) 172507.
[14] V.A. Khomchenko, D.A. Kiselev, I.K. Bdikin, V.V. Shvartsman, P. Borisov, W. Kleemann, J.M. Vieira, A.L. Kholkin, Appl. Phys. Lett. 93 (2008) 262905.
[15] W.M. Zhu, L.W. Su, Z.-G. Ye, W. Ren, Appl. Phys. Lett. 94 (2009) 142908.
[16] S. Kazhugasalamoorthy, P. Jegatheesan, R. Mohandoss, B. Karthkeran, R.J. Joseyphus, S. Dhanuskodi, J. Alloys Compd. 493 (2010) 569.
[17] J. Liu, M.Y. Li, L. Pei, J. Wang, B.F. Yu, X. Wang, X.Z. Zhao, J. Alloys Compd. 493 (2010) 544.
[18] N.V. Minh, N.G. Quan, B. Gahtori, N. Singh, H. Kishan, V.P.S. Awana, J. Alloys Compd. 509 (2011) 2663.
[19] S.Y. Chen, L.Y. Wang, H.C. Xuan, Y.X. Zheng, D.H. Wang, J. Wu, Y.W. Dou, Z.G. Huang, J. Alloys Compd. 506 (2010) 537.
[20] J. Andrés, M. Cagigas, D.S. Candela, E. Baggio-Saitovitch, J. Phys. Conf. Ser. 200 (2010) 012134.
[21] G. Le Bras, D. Colson, A. Forget, N. Genand-Riondet, R. Tourbot, P. Bonville, Phys. Rev. B 80 (2009) 134417.
[22] F.Z. Qian, J.S. Jiang, S.Z. Guo, D.M. Jiang, W.G. Zhang, J. Appl. Phys. 106 (2009) 084312.
[23] D. Kan, L. Pálová, V. Anbusathaiah, C.J. Cheng, S. Fujino, V. Nagarajan, K.M. Rabe, I. Takeuchi, Adv. Funct. Mater. 20 (2010) 1108.
[24] R.D. Shannon, Acta Crystallogr. (1976) 751, A32.
[25] P.A. Joy, P. Thakuria, Appl. Phys. Lett. 97 (2010) 163504.
[26] V.R. Palkar, D.C. Kundaliya, S.K. Malik, S. Bhattacharya, Phys. Rev. B 69 (2004) 212102.
[27] Y.P. Wang, L. Zhou, M.F. Zhang, X.Y. Chen, J.M. Liu, Z.G. Liu, Appl. Phys. Lett. 84 (2004) 1731.
[28] M. Beck, M. Ellner, E.J. Mittemeijer, Acta Mater. 49 (2001) 985.
[29] G. Huang, Y. Zhu, J. Phys. Chem. C 111 (2007) 11952.
[30] S.M. Selbach, T. Tybell, M.A. Einarsrud, T. Grande, Chem. Mater. 21 (2009) 5176.
[31] L.H. Yin, W.H. Song, X.L. Jiao, W.B. Wu, X.B. Zhu, Z.R. Yang, J.M. Dai, R.L. Zhang, Y.P. Sun, J. Phys. D: Appl. Phys. 42 (2009) 205402.
[32] A. Singh, V. Pandey, R.K. Kotnala, D. Pandey, Phys. Rev. Lett. 101 (2008) 247602.
[33] G. Catalan, Appl. Phys. Lett. 88 (2006) 102902.
[34] J. Dho, X. Qi, H. Kim, J.L. MacManus-Driscoll, M.G. Blamire, Adv. Mater. 18 (2006) 1445.
[35] X. Xiao, J. Zhu, Y. Li, W. Luo, B. Xu, L. Fan, F. Ren, C. Liu, C. Jiang, J. Phys. D 40 (2007) 5775.
[36] G.D. Hu, S.H. Fan, C.H. Yang, W.B. Wu, Appl. Phys. Lett. 92 (2008) 192905.
[37] J.F. Scott, C.A. Paz de Araujo, Science 246 (1989) 1400.
[38] H.M. Jang, J.H. Park, S. Ryu, S.R. Shannigrahi, Appl. Phys. Lett. 93 (2008) 252904.
[39] D.H. Wang, W.C. Goh, M. Ning, C.K. Ong, Appl. Phys. Lett. 88 (2006) 212907.